A&A 453, 181–191 (2006)
DOI: 10.1051/0004-6361:20054737

Astronomy & Astrophysics

Turbulence and particle acceleration in collisionless supernovae remnant shocks

I. Anisotropic spectra solutions

G. Pelletier[1], M. Lemoine[2], and A. Marcowith[3]

[1] Laboratoire d'Astrophysique de Grenoble, CNRS, Université Joseph Fourier II, BP 53, 38041 Grenoble, and Institut Universitaire de France, France
e-mail: Guy.Pelletier@obs.ujf-grenoble.fr
[2] Institut d'Astrophysique de Paris, UMR 7095 CNRS, Université Pierre & Marie Curie, 98bis boulevard Arago, 75014 Paris, France
e-mail: lemoine@iap.fr
[3] Centre d'Études Spatiales et du Rayonnement, CNRS, Université Paul Sabatier, 9 avenue du Colonel Roche, 31028 Toulouse Cedex, France
e-mail: Alexandre.Marcowith@cesr.fr

Received 20 December 2005 / Accepted 16 March 2006

ABSTRACT

This paper investigates the nature of the MHD turbulence excited by the streaming of accelerated cosmic rays in a shock wave precursor. The two recognised regimes (non-resonant and resonant) of the streaming instability are taken into account. We show that the non-resonant instability is very efficient and saturates through a balance between its growth and non-linear transfer. The cosmic-ray resonant instability then takes over and is quenched by advection through the shock. The level of turbulence is determined by the non-resonant regime if the shock velocity $V_{\rm sh}$ is larger than a few times $\xi_{\rm CR}\, c$, where $\xi_{\rm CR}$ is the ratio of the cosmic-ray pressure to the shock kinetic energy. The instability determines the dependence of the spectrum with respect to $k_\parallel$ (wavenumbers along the shock normal). The transverse cascade of Alfvén waves simultaneously determines the dependence in $k_\perp$. We also study the redistribution of turbulent energy between forward and backward waves, which occurs through the interaction of two Alfvén and one slow magneto-sonic wave. Eventually the spectra at the longest wavelengths are found almost proportional to $k_\parallel^{-1}$. Downstream, anisotropy is further enhanced through the compression at shock crossing.

Key words. acceleration of particles – shock waves – turbulence – ISM: supernova remnants

1. Introduction

Fermi acceleration of cosmic rays in astrophysical shock fronts depends in a crucial way on their transport properties in the turbulent magnetic field on both sides of the shock. Often the turbulent field spectrum and intensity are arbitrarily prescribed, assuming that it has been built by the ambient medium independently of the shock acceleration process. However Lerche (1967), Wentzel (1969) have argued for a long time that the development of an anisotropy of the cosmic ray distribution function triggers an instability upstream of the shock. McKenzie & Völk (1982) have investigated the consequences of this phenomenon in the energy budget of the shock, in particular, with respect to the efficiencies of conversion of the kinetic energy into thermal, turbulent magnetic and cosmic ray energies. Recently, Bell & Lucek (2001) have shown that the amplification of the turbulent magnetic energy could be quite significant, producing a magnetic field intensity suitable to push the high energy cut-off of the proton distribution up to the "knee" of the cosmic ray spectrum ($E \sim 3 \times 10^{15}$ eV).

This theory has then been developed further with accurate investigations of supernovae remnants (SNR). In particular Ptuskin & Zirakshvili (2003) have analysed the generation of turbulence and emphasized the importance of advection for the saturation of the spectrum. They have also carried out a preliminary examination of the role of the Kolmogorov cascade in the energy transfer among the excited waves. More recently Bell (2004) described a non-resonant regime of the streaming instability and has shown that its growth rate should be dominant in the high wavenumber range (to be discussed in more detail below). The fast growth of non-resonant modes could provide the necessary magnetic field intensity during the early stages of the SNR evolution to accelerate cosmic rays even up to the cosmic-ray spectrum "ankle" at $E \sim 3 \times 10^{18}$ eV. If verified this possibility would bring a strong support to the standard galactic cosmic-ray model (see the discussion in Drury et al. (2001) and references therein).

In this paper, we analyze the excitation of Alfvén waves as a function of the location in the upstream flow and of the wavenumber taking into account the two instability regimes (Sect. 2). In Sects. 3 and 4, we calculate the saturation mechanism of the instability considering the advection effect as a function of the wavenumber and the location in the upstream flow. We calculate the contributions of two non-linear effects: the transverse non-linear transfer among turbulent Alfvén waves, and the non-linear backscattering of Alfvén waves off slow magneto-sonic waves. These two processes are shown to be relevant and essential to the determination of the anisotropic turbulence spectra. We finally derive these spectra which are essential to calculate the cosmic-rays transport coefficients. The detailed calculation of these transport coefficients is carried out in the companion paper (Marcowith et al. 2006), hereafter Paper II. In Sect. 5, we examine the consequences in the downstream flow of the upstream excitation of the turbulence. In particular we propose a spectrum for the turbulent magnetic field and estimates of the relaxation length and of the parameters describing the dynamo action downstream. The technical derivations are presented in two appendices.

2. Upstream excitation of MHD turbulence

The instability triggered by the super-Alfvénic flow of cosmic rays upstream of a shock has been analyzed in two ways: one is related to the resonant interaction of the cosmic rays with the Alfvén waves (McKenzie & Völk 1982) and is essentially described by a kinetic theory. The other one has been recently proposed by Bell (2004) and emphasized the importance of non-resonant interactions, in which the DC-electric current of cosmic-rays generates a Lorentz force responsible for the amplification of the MHD perturbations. In fact, this is the return current in the background plasma which generates the perturbations under some conditions. Both resonant and non-resonant interactions are actually two regimes of the *same* streaming instability.

2.1. The non-resonant regime of the instability

The idea developed by Bell (2004) states that the cosmic-ray fluid weakly responds to perturbations of wavelengths shorter than their Larmor radii, so that the main response is in the form of a perturbed current of the background plasma. Actually, the major role played by the cosmic rays is to generate a DC return current in the plasma. Because there are resonant interactions with cosmic-rays of Larmor radius $r_{\rm L}$ at MHD scales k such that $kr_{\rm L}(\epsilon) = 1$, the validity criteria for the dominance of non-resonant interactions needs to be analysed carefully. Indeed, if one states that it holds for wavelengths shorter than the shortest CR-Larmor radius, then one has to pay attention to the possibility of going beyond the validity of MHD description, requiring $k\delta_0 < 1$ where $\delta_0 \equiv V_{\rm A}/\omega_{\rm ci}$.

Let us first reformulate the calculation performed by Bell (2004) as follows. The plasma remains locally neutral, so that the electric charge carried by the cosmic rays is balanced by an electric charge carried by the background plasma; n_0 being the number density of electrons or protons, the number density of protons in the cosmic ray component is $\chi_{\rm p} n_0$ ($\chi_{\rm p} < 1$) and the electrons contribute to the CR-population with a number density $\chi_{\rm e} n_0$ ($\chi_{\rm e} < 1$); the charge density in the CR-population is therefore $\rho_{\rm CR} = (\chi_{\rm p} - \chi_{\rm e}) n_0 e$. Similarly, the electric current generated by the Fermi process upstream is balanced by an electric current in the thermal plasma; thus we state that $\rho_{\rm CR} + \rho_{\rm pl} = 0$ and $\boldsymbol{J}_{\rm CR} + \boldsymbol{J}_{\rm pl} = \boldsymbol{0}$, and $J_{\rm CR} = (\chi_{\rm p} - \chi_{\rm e}) n_0 e V_{\rm sh}$ with respect to the upstream medium, $V_{\rm sh}$ being the shock velocity. Therefore, the electron component of the thermal plasma drifts with respect to the ion fluid with velocity $\boldsymbol{V}_{\rm d} = \frac{\chi_{\rm p}-\chi_{\rm e}}{1-\chi_{\rm e}} \boldsymbol{V}_{\rm sh}$. This drift does not destabilise the slow magneto-sonic waves as long as it remains smaller than the sound velocity $c_{\rm s}$, which holds when the CR-population is sufficiently tenuous that $(\chi_{\rm p} - \chi_{\rm e})/(1 - \chi_{\rm e}) < \mathcal{M}^{-1}$ ($\mathcal{M} = V_{\rm sh}/c_{\rm s}$ is the shock Mach number). When the drift velocity exceeds the instability threshold, the fast growth of magneto-sonic modes generates an anomalous resistivity that diminishes the current down to a value close to the threshold value. Or in a more explicit way, the magneto-sonic waves are amplified at a rate proportional to $V_{\rm d} - c_{\rm s}$ when the drift velocity of the thermal electrons exceeds the sound velocity. The electrons are scattered by these waves through Landau resonant interactions and thus undergo an effective collision frequency proportional to the energy of the waves. This gives rises to an anomalous resistivity that tends to reduce the electric current as the wave amplitude grows and thus to make the drift velocity $V_{\rm d}$ decrease to a value close to the sound velocity.

Hereafter, we assume for simplicity that the magnetic field lies along the shock normal. The generalization of our results to oblique situations is straightforward, as long as a de Hofmann-Teller transformation is possible.

In the non-resonant regime of the streaming instability, the cosmic-ray fluid is, in a first approximation, passive: only the thermal plasma responds while experiencing a Lorentz force due to its charge $\rho_{\rm pl}$ and its current $\boldsymbol{J}_{\rm pl}$, under the frozen in condition of the magnetic field, namely $\boldsymbol{E} + \boldsymbol{u} \times \boldsymbol{B} = \boldsymbol{0}$; where $\boldsymbol{u}$ is the local fluid velocity.

The Alfvén wave equation is then modified as follows:

$$\frac{\partial^2}{\partial t^2}\boldsymbol{u} - V_{\rm A}^2 \frac{\partial^2}{\partial z^2}\boldsymbol{u} = \rho_{\rm pl}\frac{\boldsymbol{B}_{\rm o}}{\rho_0} \times \left(\frac{\partial}{\partial t}\boldsymbol{u} + V_{\rm sh}\frac{\partial}{\partial z}\boldsymbol{u}\right). \tag{1}$$

This leads to two dispersion relations for right and left modes, namely:

$$\omega^2 - k_\parallel^2 V_{\rm A}^2 \pm k_{\rm c} V_{\rm A}^2 \left(k_\parallel - \frac{\omega}{V_{\rm sh}}\right) = 0, \tag{2}$$

where

$$k_{\rm c} \equiv \frac{|\rho_{\rm pl} B_{\rm o} V_{\rm sh}|}{\rho_0 V_{\rm A}^2} = |\chi_{\rm p} - \chi_{\rm e}| \frac{e B_{\rm o}}{m_p V_{\rm A}} \frac{V_{\rm sh}}{V_{\rm A}}, \tag{3}$$

and $\rho_0 = m_p\, n_0$.

The magnetic field $B_{\rm o}$ and the Alfvén velocity $V_{\rm A} = B_{\rm o}/\sqrt{\rho_0\, \mu_0}$ are to be considered as mean values. The scale $k_{\rm c}^{-1}$ must be compared to the minimum MHD scale $\delta_0 \equiv V_{\rm A}/\omega_{\rm ci} = c/\omega_{\rm pi}$, below which MHD no longer applies, and one gets $k_{\rm c}\delta_0 = |\chi_{\rm p} - \chi_{\rm e}| V_{\rm sh}/V_{\rm A}$. From the previous dispersion relations, we easily deduce that the waves are stable when $V_{\rm sh} < V_{\rm A}$, and that they become unstable only when $V_{\rm sh}$ is sufficiently larger than $V_{\rm A}$ and $k_\parallel < k_{\rm c}$. Indeed for $V_{\rm A}/V_{\rm sh} \ll 1$, one of the branch is unstable when $\omega^2 = -V_{\rm A}^2 (k_\parallel k_{\rm c} - k_\parallel^2) < 0$. This unstable mode is of right or left circular polarization depending on the main composition of the CR-fluid and the orientation of the magnetic field. Let $\boldsymbol{b}$ be the unitary vector that points toward the same direction as the vector $-(\chi_{\rm p} - \chi_{\rm e})\boldsymbol{B}_{\rm o}$; then one gets $\boldsymbol{u} = {\rm i}\boldsymbol{b} \times \boldsymbol{u}$: the mode is thus of right circular polarization with respect to the direction defined by $\boldsymbol{b}$. For the likely case of a proton dominated CR-fluid, the mode is left-handed with respect to $\boldsymbol{B}_{\rm o}$; in other words, it rotates in the same sense as the protons. Such a left mode exists only for $k\delta_0 \ll 1$, otherwise it is heavily damped by resonant cyclotron absorption.

Modification of the instability due to the CR-response

Following Bell's formulation, the modification is described by the complex factor $\sigma_*(k)$ such that

$$\omega^2 - k_\parallel^2 V_{\rm A}^2 \pm V_{\rm A}^2 k_{\rm c} k_\parallel (1 - \sigma_*) = 0, \tag{4}$$

where corrections in $V_{\rm A}^2/V_{\rm sh}^2$ were neglected and σ_* reads:

$$\sigma_* \equiv \frac{1+\varepsilon}{\lambda_*^{1+\varepsilon}} \int_0^{\lambda_*} \lambda^\varepsilon \sigma_{\rm p}(\lambda) {\rm d}\lambda. \tag{5}$$

In this work, we assume a CR distribution function $f(p) \propto p^{-4-\varepsilon}$ between p_0 and $p_{\max}$, where ε may be either positive or negative (see Paper II, Marcowith et al. 2006); moreover

$$\sigma_{\rm p}(\lambda) = \frac{4}{3}\lambda(1-\lambda^2)\left[\ln\left(\frac{1+\lambda}{1-\lambda}\right) + {\rm i}\pi\right] + \frac{3}{2}\lambda^2, \tag{6}$$

with $\lambda \equiv [k_{\|} r_{\rm L}(p)]^{-1}$ and $\lambda_* \equiv (k_{\|} r_*)^{-1}$ where $r_* \equiv r_{\rm L}(p_*)$. Here p_* (r_*) sets the minimum momentum (Larmor radius) of the cosmic-ray distribution function. This cut-off depends in principle on the distance x to the shock front (measured along the shock normal), since the cosmic ray distribution function roughly decreases as $f(p,x) \propto \exp[-x/\ell_{\rm D}(p)]$; $\ell_{\rm D}(p) = (1/3)c\tau_{\rm s}(p)c/V_{\rm sh}$ is related to the scattering time $\tau_{\rm s}(p)$ and is an increasing function of p. Hence at each distance x there exists $p_*(x)$, defined by $x = \ell_{\rm D}(p_*)$, such that the contribution of the smaller energies $p < p_*$ is negligible, since the corresponding diffusion lengths are short. The cosmic-ray density is $n_{\rm CR} = \int_{p_0}^{p_{\max}} {\rm d}^3 p f(p)$ is related to the CR pressure at the shock front via $n_{\rm CR} = 3P_{\rm CR}/(\Phi p_0 c)$, with Φ a dimensionless number of order $\log(p_{\max}/m_{\rm p}c) \sim 10$.

For short waves, $k \gg 1/r_*$ or $\lambda_* \ll 1$, $\Re e\{\sigma_*\} \simeq 0$ and the previous result of Eq. (2) holds. In particular, the non-resonant growth rate is

$$G_{\rm n-res}(k_{\|}) \simeq V_{\rm A}(k_{\rm c} k_{\|})^{1/2} \tag{7}$$

for $1/r_* \ll k_{\|} \ll k_c$. Note that this non-resonant instability is not operative for a wavenumber $k_{\|}$ at distances $x \ll \ell_{\rm D}(r_{\rm L} = 1/k_{\|})$ since the corresponding $r_*(x) \ll 1/k_{\|}$, r_* being an increasing function of x. The exact spatial dependence of the growth rate will be specified further on. The cut-off wavenumber $k_{\rm c}$ is redefined from the Eq. (3) by:

$$k_{\rm c} = \frac{4\pi n_{\rm CR} e V_{\rm sh}}{B_o} = \frac{12\pi}{\Phi}\frac{P_{\rm CR}}{B_o^2}\frac{V_{\rm sh}}{c}\frac{1}{r_*}\cdot \tag{8}$$

For long waves, $k \ll 1/r_*$ or $\lambda_* \gg 1$, $\Re e\{\sigma_*\} = 1$ and the CR-response dominates, i.e. the non-resonant instability is inactive.

2.2. The resonant regime of the instability

The imaginary part of σ_* describes the resonant interaction between cosmic rays and Alfvén waves; it is responsible for a growth rate that reaches a maximum for $\lambda_* = 1$, and for longer waves ($\lambda_* > 1$), $\Im m\{\sigma_*\} = \frac{3\pi}{16}\frac{1+\varepsilon}{\lambda_*^{1+\varepsilon}}$. However we will adopt a slightly different description, in the sense that we expect to get oblique Alfvén waves that essentially are of linear polarisation, which changes the resonance conditions as both electrons and ions, moving forward or backward, can resonate either with forward modes or backward modes. The small instability growth rate is the same, within an angular factor of order unity, and is given by

$$G_{\rm res}(k_{\|}, x) = G_0(k_{\|}, x)\phi(x/\ell_{\rm D}(k_{\|})), \tag{9}$$

where $\ell_{\rm D}(k_{\|})$ should be understood as $\ell_{\rm D}(r_{\rm L} = 1/k_{\|})$; the exact spatial dependence of ϕ will be specified further on. The growth rate G_0 is given by

$$G_0(k_{\|}, x) = \frac{\pi}{4}\frac{\alpha_0(\varepsilon)}{\delta_0}\frac{n_{\rm CR}}{n_0}\left(\frac{\cos\theta}{|\cos\theta|}V_{\rm sh} - \frac{4+\varepsilon}{3}V_{\rm A}\right)(k_{\|} r_*)^{1+\varepsilon}, \tag{10}$$

this expression can be found in Melrose (1986), the coefficient

$$\alpha_0(\varepsilon) = \frac{1}{2}(1+\varepsilon)(4+\varepsilon)\int |\mu|^{1+\varepsilon}(1-\mu^2)\,{\rm d}\mu.$$

Equation (10) scales as $\overline{B}^{-(1+\varepsilon)}$ similarly to Ptuskin & Zirakshvili (2003). It clearly shows that only modes propagating forward are destabilized when $V_{\rm sh}$ is sufficiently larger than the Alfvén velocity. The resonant growth rate is maximum at the scale r_* and scales like $r_*^{1+\varepsilon}$ in regards to the distance to shock front x. Note that the backward waves are damped at the same rate than the forward waves are amplified. The original calculation has been done by Lerche (1967), Wentzel (1969) and used in the theory of cosmic ray transport by Skilling (1975), then by McKenzie & Völk (1982) for the excitation of turbulence upstream of a shock. Hereafter we will assume for simplicity $\varepsilon = 0$, the value of this parameter will be discussed in Paper II.

The function ϕ stems from the solution of the evolution equation

$$V_{\rm sh}\frac{\partial}{\partial x}\phi + \frac{\partial}{\partial x}D\frac{\partial}{\partial x}\phi = 0 \tag{11}$$

with $\phi(0) = 1$. This function ϕ represents the spatial profile of the CR distribution function, which decreases with the characteristic scale given by the diffusion length $\ell_{\rm D} \equiv D/V_{\rm sh}$. The diffusion length depends on the Larmor radius $r_{\rm L}$, and thus the instability growth rate $G(k_{\|})$ decreases with ϕ with a characteristic length which is the diffusion length for $r_{\rm L} \simeq k_{\|}^{-1}$. This can be derived rigorously from the general expression of the growth rate that involves a resonance for $k_{\|} r_{\rm L}\mu = 1$ (μ is the particle pitch-angle cosine). In the case of uniform diffusion coefficient D, $\phi = \exp(-x/\ell_{\rm D})$.

3. Saturation mechanism and stationary spectra

3.1. The main elements of the theoretical description

WKB-approximation

The turbulence spectrum is not homogeneous but grows when approaching the shock front like the cosmic ray distribution. The scale of spatial variation is given at each energy by the diffusion length $\ell_{\rm D} \equiv (1/3)(c/V_{\rm sh})c\tau_{\rm s}$, which is much larger than the Larmor radius at the same energy; $\tau_{\rm s} > t_{\rm L}$ is the scattering time defined further below as a function of the turbulence spectrum. Since the mode, that undergoes a resonant interaction at this energy, has a wavelength equal to $2\pi r_{\rm L}$, its wavelength is shorter than the diffusion length and thus a WKB description of the evolution of the spectrum is suitable. This statement is also true for the non-resonant modes.

Advection versus non-linear coupling

For each spatial scale (or each value of $k_{\|}$), there are three relevant time scales: i) the growth time scales of the resonant and non-resonant modes $G_{\rm res}(k_{\|}, x)^{-1}$ and $G_{\rm n-res}(k_{\|}, x)^{-1}$, ii) the non-linear time scale that can be defined as the eddy turn over time $\tau_{\rm n-lin}(k) = (k\bar{u}(k))^{-1}$, where the turbulent velocity $\bar{u}(k)$ is such that $\rho_0\bar{u}(k)^2$ is the turbulent energy density at that scale, or by an appropriate non-linear scattering time; iii) the advection time $\tau_{\rm adv}(k)$ at which the mode is caught up by the shock front that propagates faster than the forward waves ($V_{\rm sh} > V_{\rm A}$).

The time scale $\tau_{\rm adv}(k_{\|}) = \ell_{\rm D}(k_{\|})/V_{\rm sh}$ with $k_{\|} r_{\rm L} = 1$ and one obtains

$$\tau_{\rm adv} = \frac{1}{3}\frac{c^2}{V_{\rm sh}^2}\tau_{\rm s}(1/k_{\|}). \tag{12}$$

The pitch angle frequency $\nu_{\rm s} = \tau_{\rm s}^{-1}$ is known for an isotropic spectrum $S(k)$, and, if furthermore the spectrum is a power law of the form $\eta k_{\min}^{-1}(k/k_{\min})^{-\beta}$, then

$$\nu_{\rm s} \simeq \pi(\beta-1)\omega_{\rm L}\eta\rho^{\beta-1}, \tag{13}$$

with the rigidity defined as $\rho \equiv k_{\min} r_{\rm L}$ (see Casse et al. 2002). In the above equation, the prefactor $\beta - 1$ should be replaced by $[\log(k_{\max}/k_{\min})]^{-1}$ if $\beta = 1$. The turbulence level η is defined in the next paragraph.

However, we deal with anisotropic spectra of the form $S_{3\rm d} \propto k_\perp^{-q} k_\parallel^{-\beta}$ with $q > 2$, leading to the same formula Eq. (13) (see Paper II, for further details). Hereafter, we will use 1D-spectra $S(k_\parallel)$ defined such that

$$S_{3\rm d}(\boldsymbol{k}) = 2\pi(q-2)k_{\min}^{-2}\left(\frac{k_\perp}{k_{\min}}\right)^{-q} S(k_\parallel), \quad (14)$$

which implies notably

$$\int \frac{{\rm d}^3 k}{(2\pi)^3}\, S_{3\rm D}(k) = \int \frac{{\rm d}k_\parallel}{2\pi}\, S(k_\parallel). \quad (15)$$

For convenience, hereafter, the normalization of S is defined in regards to the magnetic energy density at the infinity

$$\int \frac{{\rm d}k_\parallel}{2\pi}\, S(k_\parallel) = \int {\rm d}\log(k_\parallel)\frac{\delta B^2(k_\parallel)}{B_\infty^2} = \frac{\delta B^2}{B_\infty^2}, \quad (16)$$

where δB is the turbulent field amplitude, and B_∞ the (original) uniform component to be taken in the interstellar medium far upstream of the forward SN shock. The Alfvén velocity $V_{\rm A\infty}$ in the interstellar medium can then be deduced immediately. The magnetic field and Alfvén velocity amplified by the streaming instability are hereafter noted $\overline{B}$ and $\overline{V}_{\rm A}$. The two Alfvén velocities are linked by $\overline{V}_{\rm A} = V_{\rm A\infty}/(1-\eta)^{1/2}$ (see Ptuskin & Zirakshvili 2003). The quantity $\eta \equiv \delta B^2/(\delta B^2 + B_\infty^2)$ determines the strength of turbulence; in particular $\eta \to 1$ corresponds to $\delta B/B_\infty \to +\infty$. Finally, the magnetic field turbulent amplitude at a scale $k_\parallel$ and the 1D spectrum $S(k_\parallel)$ are tied by the relation: $\delta B^2(k_\parallel) = B_\infty^2\, k_\parallel S(k_\parallel)/(2\pi)$.

While considering the resonant instability, we distinguish the forward 1D-spectrum S^+ of forward waves and the spectrum S^- of backward waves. The pitch angle frequency is the sum of the two contributions because particles resonantly interact with both spectra irrespectively of direction of motion (this is an important point related to the resonance condition with linearly polarized Alfvén waves, as mentioned before). The advection time is using the definition of $\nu_{\rm s}$ in Eq. (13)

$$\tau_{\rm adv}(k_\parallel) = \frac{2}{3}\frac{c}{V_{\rm sh}^2}\frac{1}{k_\parallel^2}\frac{1}{S^+ + S^-}\frac{1}{1-\eta}\cdot \quad (17)$$

Note that the advection time remains finite when the magnetic field tends to be completely turbulent, i.e. when $\eta \to 1$.

We introduce an important dimensionless quantity that measures the ratio of advection time to instability growth time: $a(k_\parallel) \equiv 2G\tau_{\rm adv}$. For the resonant regime of the instability using Eqs. (10) and (17) we obtain:

$$a_{\rm res}(k_\parallel, x) = \frac{\pi}{\Phi}\mathcal{M}_{\rm A\infty}\xi_{\rm CR}\frac{1}{k_\parallel(S^+ + S^-)}\frac{\overline{B}}{B_\infty}, \quad (18)$$

where $\mathcal{M}_{\rm A\infty} = V_{\rm sh}/V_{\rm A\infty}$ is the Alfvénic Mach number measured with respect to the interstellar magnetic field value, $\xi_{\rm CR} \equiv P_{\rm CR}/\rho_0 V_{\rm sh}^2$ is the ratio of CR to shock pressure and can reach values as high as 0.5 in non-linear acceleration models (Berezhko et al. 1996; Berezhko & Ellison 1999), and $\overline{B}^2 \equiv \delta B^2 + B_\infty^2$.

The ratio $\overline{B}/B_\infty$ stems from the spatial dependence of r_* in Eq. (10) and from the $1-\eta$ factor in Eq. (17); $\overline{B}/B_\infty$ depends only on the distance to the shock front. The Eq. (18) accounts for the amplification of the magnetic field along the normal to the shock front and permits the inclusion of both non-resonant and resonant regimes in the evolution equation (see Appendices A and B). We define the reference spectrum $S_\star(k_\parallel)$

$$S_\star(k_\parallel) = \frac{\pi}{\Phi}\mathcal{M}_{\rm A\infty}\xi_{\rm CR}\frac{1}{k_\parallel}\frac{\overline{B}}{B_\infty}\cdot \quad (19)$$

Simultaneously the Alfvénic turbulence develops an energy transfer mainly in the transverse direction which determines the shape of the transverse spectrum in $k_\perp$. The non-linear transfer rate is $t_{\rm n-lin}^{-1} \approx k_\perp\, \bar{u}_\perp \simeq k_\perp\, V_{\rm A\infty} \times [k_\parallel\, k_\perp^2 S_{3\rm D}(k_\parallel, k_\perp)]^{1/2}$. We can define the efficiency of the energy transfer process using Eq. (16) and the dimensionless number $\kappa_{\rm A}$

$$\kappa_A \equiv \frac{\tau_{\rm adv}}{\tau_{\rm n-lin}} \sim \frac{c\overline{V}_{\rm A}}{V_{\rm sh}^2}\frac{1-\eta}{\eta}\cdot \quad (20)$$

This number is sufficiently high for the Alfvénic cascade to fully develop; this will be discussed in Sect. 3.3. Because the Alfvénic cascade does not convert energy from the forward waves into backward waves, the backscattering of Alfvén waves off slow magneto-sonic waves will also be considered and will proved to be efficient to redistribute the energy over all the spectra. This discussion is postponed to Sect. 4.

3.2. The spatial profiles and spectra

As mentioned earlier, the quantity $r_*(x)$ denotes the minimum Larmor radius of streaming cosmic rays at a distance x from the shock front; $r_*(x)$ can be defined by the condition:

$$\int_0^x \frac{{\rm d}x'}{\ell_{\rm D}[x', r_*(x')]} = 1, \quad (21)$$

which, if $\ell_{\rm D}$ does not depend on x, amounts to $x = \ell_{\rm D}[r_*(x)]$.

The non resonant regime of instability occurs for modes such that $k_\parallel r_*(x) \gg 1$, hence at distances $x > x_{\min}(k_\parallel)$ with $x_{\min}(k_\parallel)$ defined by $r_*[x_{\min}(k_\parallel)] = 1/k_\parallel$. Of course, this non-resonant growth occurs provided there exists cosmic rays with $r_{\rm L} > r_*(x)$, hence for $x < x_{\max} \sim \ell_{\rm D}(r_{\rm L,max})$. In contrast, the resonant interaction growth rate is maximal for $k_\parallel = 1/r_*(x)$, therefore the vicinity of the shock front $x < x_{\min}(k_\parallel)$ is dominated by the resonant regime of the instability.

In Fig. 1 we sketch the simultaneous evolution of the turbulence spectra as determined as a function of x and $k_\parallel$ and the distribution function of cosmic rays as a function x for two values of the momenta (hence two values of the Larmor radius). At point x_2, far from the shock front located at $x = 0$, only the non-resonant instability has been active in the momentum range $r_\star^{-1}(x_2) \le k_\parallel \le k_{\rm c}(x_2)$ and has produced a spectrum $S \propto k_\parallel^{-2}$ (Sect. 3.2.1). At point x_2 as there are no cosmic rays with Larmor radii such that the resonance condition $k_\parallel r_{\rm L} \sim 1$ can be satisfied in the above momentum range, since $r_\star(x_2)$ is by definition the minimum Larmor radius of cosmic rays at point x_2. The lower graph of Fig. 1 sketches accordingly the evolution of the distribution function of cosmic-rays at momentum $p_\star(x_2)$, which corresponds to the minimum momentum of cosmic-rays at x_2, or, equivalently, to a Larmor radius $r_\star(x_2)$. The minimum momentum $p_\star$ (or Larmor radius $r_\star$) is a growing function of x, in particular $p_\star(x_2) > p_\star(x_1)$. Hence, at point x_1, the resonant instability has been active in the momentum range $k_\parallel \lesssim 1/r_\star(x_1)$ as there are cosmic-rays with Larmor radii that can satisfy the resonance condition in this range. The corresponding spectrum is

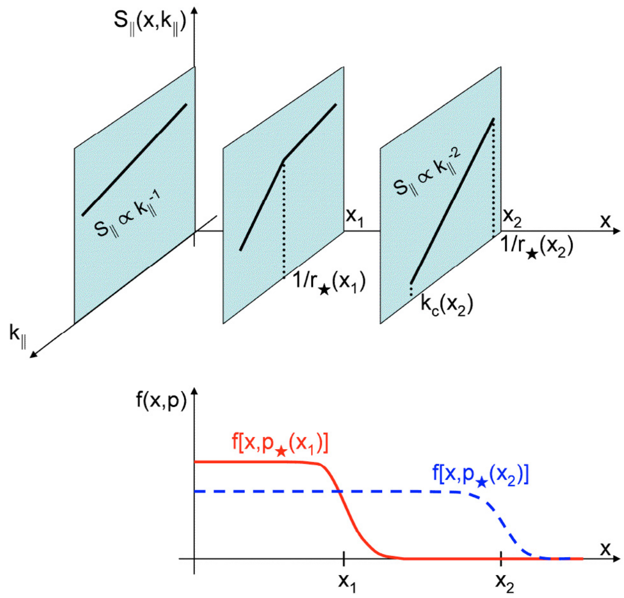

Fig. 1. Sketch of the evolution of the turbulence spectrum S in the $(x, k_\parallel)$ plane (*upper graph*) and of the cosmic-ray distribution function $f(x, p)$ as a function of x for two values of the momenta (*lower graph*). See text for details.

$S \propto k_\parallel^{-1}$ (Sect. 3.2.2). At momenta $k_\parallel \gtrsim 1/r_\star(x_1)$, only the non-resonant instability has been active, for reasons similar to those discussed above, and therefore the spectrum $S \propto k_\parallel^{-2}$. Finally, at the shock front, the resonant instability has overtaken the non-resonant instability over all the wavelength range, so that the final spectrum $S \propto k_\parallel^{-1}$.

Since the two regimes of the instability take place in different regions, we can solve for the spectra using in a first place the equation involving solely non-resonant growth for $x_{\min}(k_\parallel) < x < x_{\max}$ and then use this solution at $x_{\min}(k_\parallel)$ as the initial condition for resonant growth up to the shock front at $x = 0$.

3.2.1. The non-resonant regime

The equation governing the growth of the turbulent spectrum through the non-resonant instability is, using Eq. (7):

$$V_{\rm sh}\frac{\partial}{\partial x}S(k_\parallel, x) = -2V_{A\infty}\sqrt{k_c(x)k_\parallel}\,\theta(x_{\max}-x)S(k_\parallel, x), \quad (22)$$

where $k_c(x)$ is defined in Eq. (27). Assuming for the moment that η is constant ($=\eta_\infty$), Eq. (21) then gives $x = \ell_D(r_*)$, or:

$$k_{\min} r_*(x) \simeq \left(\frac{3\eta_\infty V_{\rm sh}}{c}\right)^{1/(2-\beta_<)} (k_{\min}x)^{1/(2-\beta_<)}, \quad (23)$$

where $\beta_<$ is the index of the turbulent spectrum in the vicinity of the shock front, i.e. that which is produced by the resonant instability. Introducing

$$\zeta \equiv \frac{2}{(3\eta_\infty)^{1-m}}\mathcal{M}_{A\infty}^{-1}\left(\frac{V_{\rm sh}}{c}\right)^{m-\frac{1}{2}}\left(\frac{12\pi}{\Phi}\frac{P_{\rm CR}}{B_\infty^2}\right)^{1/2}, \quad (24)$$

with $m = (3-2\beta_<)/(4-2\beta_<)$, then

$$S(k_\parallel, x) = S(k_\parallel, x_{\max})\exp\left\{-\frac{\zeta}{m}\sqrt{\frac{k_\parallel}{k_{\min}}} \times\left[(k_{\min}x)^m - (k_{\min}x_{\max})^m\right]\right\}. \quad (25)$$

The amplification factor is thus:

$$\frac{S(k_\parallel, x=0)}{S(k_\parallel, x_{\max})} = \exp\left[\frac{\zeta}{m}\sqrt{\frac{k_\parallel}{k_{\min}}(k_{\min}x_{\max})^m}\right]. \quad (26)$$

It turns out that $k_{\min}x_{\max} = \ell_D(r_{L,\max})/r_{L,\max} \gg 1$, and for $\beta_< = 1$ (corresponding to Bohm scaling, see next section) $\zeta \sim 1$. The amplification would be enormous, the instability would deplete the shock quickly, unless another saturation mechanism occurred earlier. Even if we accounted for a variation of η, the amplification level would still be too large, as the following saturation mechanism keeps the magnetic field energy density to a lower level.

Saturation mechanism

In fact, the non-resonant growth should saturate much earlier. As the magnetic field gets amplified beyond its initial value, one can extrapolate the previous calculations by substituting $B_{<k}$ for B_∞, where $B_{<k}^2 = B_\infty^2 + \int_{k_{\min}}^{k_\parallel} {\rm dlog}\, k'_\parallel\,\delta B^2(k'_\parallel)$ represents the average field on scales larger than $k_\parallel^{-1}$, and again $\delta B(k_\parallel)$ denotes the amplified random component on scale $k_\parallel$.

For $|\chi_p - \chi_e| \sim \chi_p$, using Eq. (3), the cut-off wavenumber of the instability k_c can be written as

$$k_c = \frac{4\pi n_* e V_{\rm sh}}{B_{<k}} = \frac{12\pi}{\Phi}\frac{P_{\rm CR}}{B_{<k}^2}\frac{V_{\rm sh}}{c}\frac{1}{r_*}. \quad (27)$$

The non-resonant instability occurs for wavenumbers $1/r_* < k_\parallel < k_c$ and its saturation is achieved once $k_c r_* = 1$. This simple condition leads to a magnetic field energy density:

$$\frac{B^2}{8\pi} \simeq \frac{3}{2\Phi}\frac{V_{\rm sh}}{c}P_{\rm CR} \sim \frac{3\xi_{\rm CR}}{2\Phi}\rho_0\frac{V_{\rm sh}^3}{c}. \quad (28)$$

This last estimate is in agreement with Bell (2004).

However, the instability may also saturate through non-linear transfer effects. As the field builds up through the instability, the non-linear transfer time $t_{\rm n-lin}(k_\parallel)$ along the $k_\parallel$ direction decreases to the point where the instability saturates when $G_{\rm n-res}(k_\parallel)t_{\rm n-lin}(k_\parallel) = 1$. In order to see when this happens, one can express the non-linear transfer time as:

$$t_{\rm n-lin}(k_\parallel) = \left[k_\parallel \overline{V}_A(k_\parallel)\right]^{-1}, \quad (29)$$

with $\overline{V}_A(k_\parallel) = \delta B(k_\parallel)/\sqrt{4\pi n_0}$, and the non-resonant growth rate $G_{\rm n-res}(k_\parallel) = \sqrt{k_\parallel k_c}\,V_A$. We then find for the saturated field at a scale $k_\parallel$:

$$\delta B^2(k_\parallel) \simeq \frac{12\pi}{\Phi}P_{\rm CR}\frac{V_{\rm sh}}{c}\frac{1}{k_\parallel r_\star}. \quad (30)$$

Integrating this result over $k_\parallel r_* > 1$, we exactly obtain the same saturation level as previously, which is quite remarkable. This means that even if there is a kind of quasi-linear saturation at work, within the same time the non-linear transfer remodels the spectrum. The spectrum derived above from this remodeling process is likely correct but would require a more elaborated theory together with sophisticated numerical simulations to be confirmed.

Using Eq. (30) the non-resonant spectrum profile is thus

$$S(k_\parallel, x) = \frac{2\pi\,\delta B^2(k_\parallel)}{k_\parallel\, B_\infty^2} = \frac{3\pi}{\Phi}\xi_{\rm CR}\frac{V_{\rm sh}}{c}\frac{\rho_0 V_{\rm sh}^2}{P_{B_\infty}}\frac{1}{r_\star k_\parallel^2} \propto k_\parallel^{-2}. \quad (31)$$

We obtained this result by assuming energy transfer along the $k_\parallel$ direction. However the relevant transfer could be transverse through an Alfvén cascade, as is often considered. In this case the transfer rate $k_\perp \bar{u}$ is supposed to be faster and a balance $k_\perp \bar{u} \sim G_{\rm n-res}(k_\parallel)$ is expected. However it generally requires the prescription of a relation between $k_\perp$ and $k_\parallel$ (see Sect. 3.3). Setting $k_\perp r_\star \sim (k_\parallel r_\star)^m$ with $m \geq 1$, we obtain a spectrum

$$S(k_\parallel) \propto k_c r_\star^2 (k_\parallel r_\star)^{-2m}. \tag{32}$$

There is no clear constraint on the value of m, which may be taken to 1 without apparent inconsistency. In any case, as $m \geq 1$, the same estimate (28) of the saturation level is found, which makes this estimate fairly robust.

To draw a complete picture of the saturation spectrum, one would need to follow the evolution of non-linear turbulence transfer at the same time as the evolution of the non-resonant instability and the position dependence of $r_\star$.

3.2.2. The resonant regime

As the turbulence is advected to the shock front, cosmic rays with Larmor radius $r_{\rm L} = 1/k_\parallel$ appear and induce the resonant instability. This latter is then quenched by advection through the shock, which thus provides the main saturation mechanism of this instability.

i) For the sake of clarity, we first assume equally amplified forward and backward spectra, and $S = S^+ + S^-$. The evolution equation for this latter reads

$$\frac{\partial}{\partial x} S(k_\parallel, x) = -a_{\rm res}(k_\parallel, x) \frac{{\rm e}^{-x/\ell_{\rm d}}}{\ell_{\rm d}} S(k_\parallel, x). \tag{33}$$

The initial condition for integration lies at $x = x_{\rm min}(k_\parallel)$ and is given by the spectrum produced by the non-resonant instability. We argue that the resonant amplification will not modify the overall magnetic field strength $\overline{B}$ over that produced the non-resonant instability by a large factor for typical SNe environment and shock wave values. Hence, to solve Eq. (33) above, we first assume that the ratio $(1-\eta)^{-1}$ is constant between the shock front ($x = 0$) and the point where the resonant instability first comes into play, defined by $x = x_{\rm min}(k_\parallel)$ for $k_\parallel = k_{\rm min}$. Then $1/(1-\eta)^{1/2} = \overline{B}_*/B_\infty$ with $\overline{B}_*$ the value of $\overline{B}$ at this latter point. In this case, $\ell_{\rm D}$ does not depend on x in the interval in which the resonant instability acts, and the equation for S can be solved as:

$$S(k_\parallel, x) = S(k_\parallel, x_{\rm min}) + \frac{\tilde{\alpha}_{\rm res}}{k_\parallel}\left({\rm e}^{-x/\ell_{\rm D}} - {\rm e}^{-1}\right)\frac{\overline{B}_*}{B_\infty}, \tag{34}$$

with $\tilde{\alpha}_{\rm res} \equiv (\pi/\Phi)\mathcal{M}_{\rm A\infty}\xi_{\rm CR}$ (see Eq. (18)). The term $S_{\rm nr} \equiv S(k_\parallel, x_{\rm min})$ is the spectrum produced by the non-resonant instability and is proportional to $k_\parallel^{-2}$ due to saturation. The second term on the rhs is the contribution of the resonant instability and we denote it $S_{\rm r}(k_\parallel)$ at the shock front; it is proportional to $k_\parallel^{-1}$ and dominates the former over the whole range of wavenumbers if $a_{\rm res}\overline{B}_*/B_\infty$ is sufficiently large. In case of the absence of non-resonant instability, $\overline{B}_* = B_\infty$ and the expression of $\tilde{\alpha}_{\rm res}$ leads to a resonant saturation level (see Bell & Lucek 2001)

$$\frac{B_{\rm res}^2}{B_\infty^2} \sim \xi_{\rm CR} M_{\rm A\infty}. \tag{35}$$

The contribution of the resonant instability to the magnetic field energy density $B_{\rm res}^2/8\pi$ is obtained from:

$$\int_{k_{\rm min}}^{k_{\rm max}} {\rm d}k_\parallel\, S_{\rm r}(k_\parallel) \sim \tilde{\alpha}_{\rm res}\frac{\overline{B}_*}{B_\infty}\log\left(\frac{k_{\rm max}}{k_{\rm min}}\right). \tag{36}$$

Hence

$$\frac{B_{\rm res}^2}{B_{\rm n-res}^2} = \frac{\pi}{\Phi}\log\left(\frac{k_{\rm max}}{k_{\rm min}}\right)\xi_{\rm CR} M_{\rm A\infty}\frac{B_\infty}{\overline{B}_*} \sim \sqrt{\frac{\xi_{\rm CR}\, c}{V_{\rm sh}}}, \tag{37}$$

this ratio is larger than one by a factor of a few for shock velocities lower than a few times $\sim\xi_{\rm CR} c$. Among other things, this implies that the scaling with $k_\parallel$ of the total spectrum at the shock front will be dominated by the resonant contribution.

One can investigate the effect of the above assumption $1/(1-\eta)$ = constant by integrating formally Eq. (33) as:

$$S(k_\parallel, x) = S(k_\parallel, x_*) + \frac{a_{\rm res}}{k_\parallel}\int_0^1 {\rm d}y\, {\rm e}^{-y}\frac{\overline{B}[x(y, k_\parallel)]}{B_\infty}, \tag{38}$$

with $y = x/\ell_{\rm d}(x)$. The integration in the rhs can be understood as a function of $k_\parallel$ so that the dependence of the second term on the rhs is not strictly speaking $\propto k_\parallel^{-1}$. However $\overline{B}(x)/B_\infty$ is a decreasing function of x and therefore it is bounded by below by $\overline{B}[x_*(k_\parallel = k_{\rm min})]/B_\infty$ and by above by $\overline{B}(0)/B_\infty$. The integral in Eq. (38) is thus bounded by two constants that are independent of $k_\parallel$ and whose ratio is a factor $\overline{B}(0)/\overline{B}[x_*(k_\parallel = k_{\rm min})] \sim$ a few. Hence the integral modulates only weakly the powerlaw $\propto k_\parallel^{-1}$ and we conclude that, at the shock front, the spectrum $S \propto k_\parallel^{-1}$. It should be noted that the total variation of the magnetic field in the resonant region is even more limited if $\varepsilon > 0$ as we shall see in Paper II, as in that case $a_{\rm res}$ varies as $(\overline{B}/B_\infty)^{1-\varepsilon}$.

ii) If the backward spectrum is not amplified nor remodeled by mode coupling, the solution is similar to the previous case without the factor 2.

iii) If the backward waves are damped at the same rate as the forward waves are amplified, S^+S^- = constant. If the forward spectrum is amplified an obvious solution is obtain for $S^+ \gg S^+(x = x_{\rm min})$

$$\begin{aligned} S^+ &\simeq S_*(k_\parallel) \times (\exp(-x/\ell_{\rm d}) - {\rm e}^{-1}) \\ S^- &\simeq \frac{S^+(x = x_{\rm min}) S^-(x = x_{\rm min})}{S^+}. \end{aligned} \tag{39}$$

The backward waves are damped exponentially.

iv) The backward waves can also be generated by backscattering process of forward Alfvén waves off acoustic waves (slow magneto-sonic modes precisely). This process deserves a specific development presented in Sect. 4.

3.3. The behavior of Alfvénic turbulence

The behavior of moderate MHD turbulence – moderate in the sense that a significant mean magnetic field is preserved – is peculiar when incompressibility is assumed, because of the particularity of Alfvén waves dynamics. Resonant three wave interactions do not develop as usual dispersive waves, because of their specific dispersion relation: $\omega = k_\parallel V_{\rm A}$. However, a forward wave and an opposite backward wave can couple through a resonant interaction with a third wave with $k_\parallel = 0$ (Bhattacharjee & Ng 2001; Galtier et al. 2000). The weak turbulence description shows that the energy cascade in the inertial range occurs only in the transverse direction to the mean field. The stationary spectrum is in $k_\perp^{-3}$ and the dependence in $k_\parallel$ is arbitrary, which means that it is determined by the mechanism of generation of the turbulence. This behavior has been observed in numerical simulations even in the regime of moderate turbulence (Bhattacharjee & Ng 2001). The extension of the resonant three wave interaction by taking account of a nonlinear broadening due to the relaxation of triple correlation – the so-called Eddy Damping Quasi Normal Markovian description – has been done for MHD turbulence with a mean field by Goldreich & Sridhar (1995). They have argued that some re-organization of the spectrum occurs in $k_\parallel$ due to scaling constraints between the nonlinear transfer in the transverse direction and the parallel propagation of Alfvén waves. Let us summarize this discussion. These Alfvén waves (also called shear Alfvén waves, as opposed to MHD waves that have parallel components) are incompressible and purely transverse to the mean field. The turbulent energy density $\epsilon \propto \bar{u}_\perp^2$ and the eddy turn over time $\tau_{\rm n-lin} \sim (k_\perp \bar{u}_\perp)^{-1}$. The scale invariant spectrum of the energy cascade is unavoidably anisotropic $S_{\rm 3D}(k_\perp, k_\parallel) \propto k_\perp^{-q} k_\parallel^{-\beta}$. The critical balance assumption of Goldreich and Shridar is that the transfer rate $\tau_{\rm tr} = \tau_{\rm n-lin} \sim \tau_{\rm A}$ at all scales, where $\tau_{\rm A} = (k_\parallel V_{\rm A})^{-1}$. Then for an anisotropic inertial cascade such that the energy transfer rate at each scale is constant, namely $Q \propto \epsilon/\tau_{\rm n-lin} \propto k_\perp u_\perp^3$ = constant, a relation between parallel and transverse wavenumbers is found:

$$k_\parallel \sim \frac{Q^{1/3}}{V_{\rm A}} k_\perp^{2/3}. \tag{40}$$

In this more elaborated description (EDQNM) no energy transfer from forward waves to backward waves and vice versa takes place. Recent numerical simulations (Cho & Vishniac 2000; Maron & Goldreich 2001) have suggested that the scaling $\tau_{\rm n-lin} \propto \tau_{\rm A}$ was preserved in all regimes, so that $\tau_{\rm n-lin} = \tau_{\rm A}/\chi$, with χ a constant independent of the wavenumber at all scale, and $\tau_{\rm tr} = \tau_{\rm n-lin}/\chi$. The previous relation is thus extended to

$$k_\parallel \sim \frac{Q^{1/3}}{\chi^{4/3} V_{\rm A}} k_\perp^{2/3}. \tag{41}$$

Whereas the weak turbulence theory leads to a spectrum in $k_\perp^{-2} f(k_\parallel)$ with an arbitrary function f of $k_\parallel$, the Goldreich-Shridar theory leads to a spectrum $S_{\rm 3D} \propto k_\perp^{-q-2/3} f(k_\parallel/k_\perp^{2/3})$. When a scale invariance in $k_\parallel$ is generated in the turbulence situation, the spectrum is of the form $S_{\rm 3D} \propto k_\perp^{-q} k_\parallel^{-\beta}$. Then Eq. (41) together with the assumption of a constant energy transfer rate $Q \propto \epsilon/\tau_{\rm n-lin}$ with $\epsilon \sim k_\perp^2 k_\parallel S_{\rm 3D}$ provide a relation between the index of the parallel spectrum with the index α of the perpendicular spectrum (Galtier et al. 2005):

$$3\alpha + 2\beta = 7 \text{ with } \alpha = q - 1. \tag{42}$$

This is considered to be the generalization of Iroshnikov-Kraichnan theory (Iroshnikov 1964; Kraichnan 1965) when anisotropic effects are taken into account. Still some arbitrariness is maintained. However the CR-instability in resonant regime generates a turbulent spectrum such that $\beta = 1$, and the transverse Alfvénic couplings between modes then lead to $\alpha = 5/3$. Only couplings with slow magneto-sonic modes may allow to obtain the same spectrum for the backward waves and the slow waves.

4. Nonlinear generation of backward waves

The process $A^+ \rightarrow A^- + S^+$, where A represents Alfvénic modes and S a slow magneto-sonic mode, is the only process that can transfer energy from forward waves to backward waves and it turns out to be efficient, as will be seen further on. The frequency of the slow magneto-sonic mode is such that $\omega^{\rm s} = k^{\rm s} V_{\rm sm}(\theta_{\rm s})$; for convenience, we write it $\omega^s = \beta_{\rm s} k_\parallel^s V_{\rm A}$, where, for $c_{\rm s} < V_{\rm A}$, $\beta_{\rm s} \simeq \frac{c_{\rm s}}{V_{\rm A}}(1 + \frac{c_{\rm s}^2}{V_{\rm A}^2}\sin\theta_{\rm s})^{-1/2}$; this number is assumed smaller than unity and weakly varying with $\theta_{\rm s}$. The process is most efficient under the resonance condition: $\omega^+ - \omega^- - \omega^{\rm s} = 0$. Since the wave vectors are such that $\boldsymbol{k}^+ - \boldsymbol{k}^- - \boldsymbol{k}^{\rm s} = 0$, we obtain the following relations between the parallel wavenumbers:

$$k_\parallel^+ = k_\parallel^{\rm s} \frac{1+\beta_{\rm s}}{2} \tag{43}$$

$$k_\parallel^- = -k_\parallel^{\rm s} \frac{1-\beta_{\rm s}}{2} < 0. \tag{44}$$

Therefore, when the magnetic field is above the equipartition value (e.g. $V_{\rm A} > c_{\rm s}$), $\beta_{\rm s} < 1$, and we always get a backscattering of Alfvén waves off slow magneto-sonic modes. Backscattering would not be possible with other MHD waves, for obvious kinematic reasons. This backscattering process with Alfvén waves is analogous to the Brillouin backscattering process with usual electro-magnetic waves of the vacuum. Even if no sonic waves are excited beforehand, the primary Alfvén waves can generate them spontaneously above some threshold (see Pelletier & Kersalé 2000). In the interstellar medium $V_{\rm A} \simeq 3\, c_{\rm s}$; it is already sufficient to get the backscattering process. The domination of the Alfvén velocity over the sound speed is even increased at the external shock of SNr because of their convexity. Indeed in the shock frame, the ambient medium converges towards the front at a velocity $-\boldsymbol{V}_{\rm sh}$ that points towards the center of curvature, the density increases and therefore the frozen in magnetic field has an amplified transverse component. From the evolution equations multiplied by $\tau_{\rm adv}$, we introduce the dimensionless parameter

$$\kappa \equiv \frac{\pi}{12} \frac{c\overline{V}_{\rm A}}{\beta_{\rm s} V_{\rm sh}^2}, \tag{45}$$

which measures the importance of the backscattering process as compared to advection. Typically, κ is a number close to one.

For the most interesting cases where the backscattering process efficiently remodels the stable spectra, the asymptotic spectra, determined externally by the turbulence in the interstellar medium, can be ignored. The spectra are then proportional to $S_*(k_\parallel) k_\perp^{-q}$. Because the diffusion length is generally not constant, but dominated by the spectrum of unstable waves, for numerical simulation purpose, it is convenient to describe the profiles of the wave spectra with the help of a dimensionless variable y defined by $dx = \ell_{\rm D}(r_{\rm L} = 1/k_\parallel, x) dy$. Then the function $\phi = {\rm e}^{-y}$. We have to bear in mind that, when the problem is solved for the variable y, we can reconstruct the spectrum profile in the variable x. Since $\ell_{\rm D}(r_{\rm L} = 1/k_\parallel, x) = (1/3)(c/V_{\rm sh}) k_\parallel^{-1} (k_\parallel/k_{\rm min})^{\beta-1} \eta^{-1}(x)$, one finds:

$$y = 3\frac{V_{\rm sh}}{c}\left(\frac{k_\parallel}{k_{\rm min}}\right)^{2-\beta} \int_0^x {\rm d}x' k_{\rm min}\, \eta(x').$$

The quantity $r_*(x)$ is defined by $y = 1$ for $r_{\rm L} = r_*$, hence $y = (k_\parallel r_*)^{2-\beta}$. The regions with $y \geq 1$ ($y \leq 1$) correspond to far (close) distances to the shock front and is dominated by the non-resonant (resonant) waves. Therefore the evolution of the spectra reduces to a differential system that governs the evolution of their amplitude as a function of the y variable. As long as κ is small, the solution given by Eq. (39) is slightly modified and the order three system that describes the generation of backward A-wave and forward S-wave is sufficient (see Appendix A).

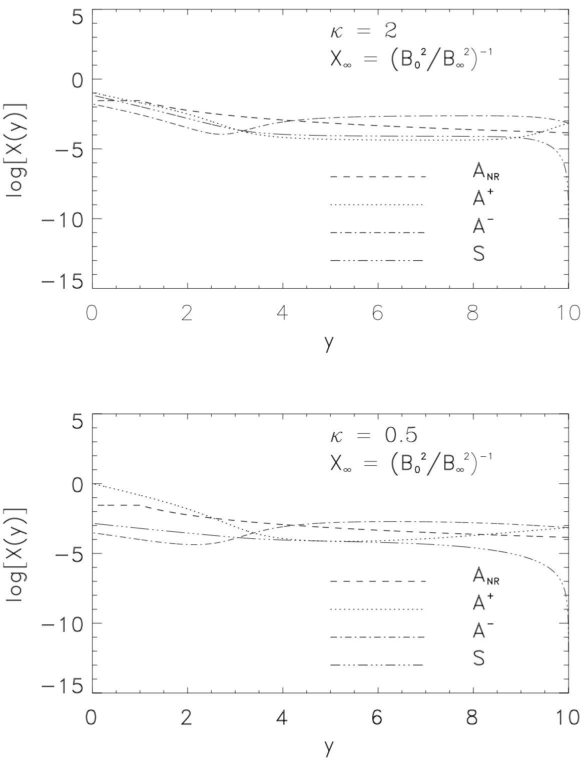

Fig. 2. Solutions of third order system for different value of the κ parameter (see the definition in the text). Even if they have been defined for y between 0 and 1, the resonant waves profiles are calculated between the shock front and $y = 10$ where they match their asymptotic interstellar values. The wave-particle resonance depends on the particle pitch-angle α, at $r_L = r_*$ we have $k_\parallel r_* \cos\alpha \simeq 1$, the product $k_\parallel r_*$ and then y can be above 1. In the upper panel, $\kappa = 1$ is high leading to a strong conversion of forward Alfvén waves into backward Alfvén waves and sound waves. For $y \leq 5$, the resonant instability takes over the non-linear transfer, the forward Alfvén waves are produced and the backward waves are pumped. The sound waves are heavily produced between $y = 5$ and the shock front. The ratio of forward to backward Alfvén waves at the shock front is about three orders of magnitude. In the lower panel $\kappa = 0.1$, the production of backward Alfvén and sound waves is less intense. In both cases the amplification factor $\overline{B}_*/B_\infty = 10$. The boundary conditions are: $X^+ = X^- = X_\infty = A^{-2} \ll 1$ and $X^s = 0$. All simulations have been performed with $\epsilon = 0$.

The numerical integration leads to the solutions sketched in Fig. 2, that shows that for, increasing κ, more and more conversion into backward A-waves and forward S-waves is realized. However when κ is increased significantly, one has to take account of the secondary process where backward A-waves decay into forward A-waves and backward S-waves. The evolution is then described by a system of order four (see Appendix B). The numerical solutions are displayed in Fig. 3. It can be that a significant backward spectrum is generated; however without changing the order of magnitude of the primary spectrum.

5. Downstream: dynamo action and turbulence relaxation

If turbulence is still moderate downstream, then the spectra built upstream are transmitted across the front, and thus a $k_\parallel^{-1}$ 1D-spectrum is maintained downstream. Bohm diffusion would then applies downstream as well.

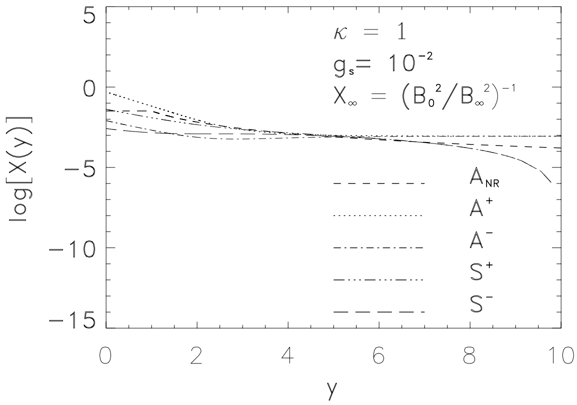

Fig. 3. Solutions of the fourth order system. The non-linear transfer parameter $\kappa = 1$ and the damping rate of sound waves is $g_s = 5 \times 10^{-3}$. This choice corresponds to a ratio $V_A/c_s = 3$. All simulations have been performed with $\epsilon = 0$. The results show that as long as the damping or growing effects do not dominate the transfer among the waves (for $y \leq 5$), the non-linear transfer mostly produce backward and forward sound waves equally. In both cases the amplification factor $\overline{B}_*/B_\infty = 10$. The boundary conditions are: $X^+ = X^- = X_\infty = A^{-2} \ll 1$, and $X^{s+} = X^{s-} = 0$.

5.1. Helicity and estimate of dynamo amplification downstream

The non-resonant regime of the streaming instability induces a left-right symmetry breaking. Therefore the turbulence carries helicity which offers grounds for dynamo action. The helicity can be calculated in term of the difference between the spectrum of right-handed modes $S_{\rm RH}$ and the spectrum of left-handed modes $S_{\rm LH}$ (the $k_\perp$ dependence has been integrated out):

$$H \equiv \langle \boldsymbol{u} \cdot \mathrm{rot}\,\boldsymbol{u} \rangle = 2V_A^2 \int (S_{\rm RH} - S_{\rm LH}) k_\parallel \frac{\mathrm{d}k_\parallel}{2\pi}. \quad (46)$$

The integrand can be considered as the helicity spectrum S_H. This spectrum is used to calculate the so-called “alpha”-parameter of the turbulent dynamo theory:

$$\alpha_D = \int \frac{\Gamma(k_\parallel)}{\omega_k^2 + \Gamma^2(k_\parallel)} S_H(k_\parallel) \frac{\mathrm{d}k_\parallel}{2\pi}, \quad (47)$$

where Γ is the damping rate of the turbulence in stationary state. In our problem the main damping mechanism is the shock advection: $\Gamma(k_\parallel) = 1/\tau_{\rm adv}(k_\parallel)$. For the non-resonant modes $\omega_k^2 \ll \Gamma^2(k_\parallel)$ and the dynamo coefficient reads:

$$\alpha_D = \frac{2}{3} c \frac{V_A^2}{V_{\rm sh}^2} \int \frac{S_{\rm RH} - S_{\rm LH}}{S^+ + S^-} \frac{1}{k_\parallel} \frac{\mathrm{d}k_\parallel}{2\pi} = \frac{2c}{3\pi} \frac{V_A^2}{V_{\rm sh}^2} \ln \frac{r_*}{r_0}, \quad (48)$$

The helicity is transfered through the shock as has been calculated by Schlickeiser (1998). Helicity in the spectrum matrix leads to a third diffusion coefficient for the cosmic rays because the two transverse space variable are correlated $\langle \Delta x_1 \Delta x_2 \rangle \neq 0$ (see Paper II).

The mean field evolves in the turbulent plasma according to the following equation:

$$\frac{\partial}{\partial t} \boldsymbol{A} = \alpha_D \boldsymbol{B} + \boldsymbol{u} \times \boldsymbol{B} + \nu_t \Delta \boldsymbol{A}, \quad (49)$$

where ν_t is the turbulent magnetic diffusivity. A typical scale for the variation of the mean field arises, namely $\ell_{\rm dyn} = \nu_t/\alpha_D$ with an associated time scale $\tau_{\rm dyn} = \ell_{\rm dyn}/u_2$. More precisely, the dynamo modes of wavelength larger than v_t/α_D grow and it is expected that the mean field reaches an intensity on the order of the equipartition value, not more.

5.2. Relaxation or compression downstream

The turbulence properties downstream (level of turbulence, spectral index) can be constrained from the size of the X-ray filaments in young SNr (see Parizot et al. 2006). It is shown that the relativistic electrons with tens of TeV energies producing the observed synchrotron radiation have a diffusion coefficient close to the Bohm value. Recently, Pohl et al. (2005) have pointed out the importance of the relaxation length of the turbulence downstream the shock. The authors stressed that the size of the X-ray filaments observed in young SNr (see the discussion in Sect. 6) may be well controled by the turbulence rather than by the synchrotron losses. However, the previous analysis has been made assuming an isotropic turbulence spectrum, which is not correct at least for two reasons: the turbulence is already anisotropic upstream and the magnetic field amplified upstream is compressed in the direction parallel to the shock front.

In order to elucidate the way the turbulence acts on relativistic particles, we compare the non-linear Alfvén transfer time $t_{\rm n-lin}(k_\parallel) = [k_\parallel \overline{V}_{\rm A}(k_\parallel)]^{-1}$

$$t_{\rm n-lin}(k_\parallel) = \frac{l_\parallel}{\overline{V}_{\rm A}\sqrt{\beta-1}}(l_\parallel k_\parallel)^{(\beta-3)/2}, \tag{50}$$

and the term $\beta - 1$ in the prefactor should be replaced by $1/\log(k_{\max}/k_{\min})$ when $\beta = 1$. The downstream return timescale reads:

$$t_{\rm ret} = \kappa\left(\frac{c}{V_{\rm s}}\right)^2 \frac{2}{3} t_{\rm s}, \tag{51}$$

$t_{\rm s} = (2\pi)^{-\beta}\eta^{-1}(l_\parallel/c)(r_{\rm L}/l_\parallel)^{2-\beta}$ being the angular scattering timescale downstream; in the above expressions, $l_\parallel$ is the coherence length in the parallel direction. The prefactor $\kappa < 1$ accounts for the shortening of the return timescale in compressed turbulence. The condition $t_{\rm ret} < t_{\rm n-lin}$ means the particle does explore distances smaller than the relaxation length of the turbulence downstream and experience a compressed rather than a relaxed turbulence during their journey downstream. In the case of Bohm type turbulence (meaning $\beta = 1$) the ratio of the two timescales translates into

$$\frac{t_{\rm ret}}{t_{\rm n-lin}} \simeq \frac{\kappa}{3\pi}\,\frac{c}{V_{\rm sh}\mathcal{M}_{\rm A\infty}}\,\frac{\log(k_{\max}/k_{\min})^{-1/2}}{(1-\eta)^{1/2}\eta}. \tag{52}$$

Using typical values of the magnetic field, mean density and shock velocity in our problem (see next section) and acknowledging for a saturation level of $\mathcal{M}_{\rm A\infty}\xi_{\rm CR}\overline{B}_*/B_\infty \simeq \eta/(1-\eta) \simeq 1/(1-\eta)$, we find a ratio $t_{\rm ret}/t_{\rm n-lin} \simeq 0.5\kappa\ (V_{\rm sh,-1}^{-1}\xi_{\rm CR}/\Phi)^{3/4}$ where $V_{\rm sh,-1}$ is the shock velocity in units of $0.1c$. The previous ratio is thus expected to be ≤ 1 unless the shock velocity is lower than $10^{-2}c$.

6. Astrophysical consequences

Supernova blast waves explore different external interstellar media (ISM) during their evolution. We consider only two phases of the SN evolution: the very early free expansion phase where the shock velocity can reach extreme values as high as $V_{\rm sh} \simeq 0.1c$ and the late free expansion phase (or early Sedov self-similar phase) where the shock velocity drops to $V_{\rm s} \simeq 10^{-2}c$. These two phases are the more relevant concerning high energy cosmic ray production. In the latter phase the remnant may expand either in a hot rarefied ($T \simeq 10^6$ K, $n \simeq 10^{-3/-2}$ cm^{-3}) interior of a massive star wind bubble or in a warm partially ionised ($T \simeq 10^4$ K, $n \simeq 10^{-1/0}$ cm^{-3}). The mean ISM magnetic field in both cases is conservatively taken to 3 μGauss. In the very early phase of the SNr evolution, the medium is probably much denser with $n \simeq 10$–100 cm^{-3}.

The ratio of the saturation magnetic field energy density of the non-resonant and resonant instability (when both regimes are present) respectively is $S_{\rm n-res}/S_{\rm res} \simeq \sqrt{V_{\rm sh}/(\xi_{\rm CR}\, c)}$. The non-resonant regime appears to dominate for the very early free-expansion phase as already pointed out by Bell (2004), while the resonant regime dominates by a factor 10–100 (see discussion in Sect. 3.2.2) in the late free-expansion phase and Sedov self-similar phases. The magnetic field deduced (only lower limits) from the size of bright X-ray filaments in young SNr (Berezhko & Völk 2004; Vink 2004; Völk et al. 2005; Parizot et al. 2006) is expected to be mostly produced in the resonant regime should then scale approximately as $\sqrt{V_{\rm sh}}$ (see Eq. (35)). We have seen above that if the non-resonant regime contributes substantially to the amplification this dependence is not as simple and the way the shock decelerates during the earlier phases can modify it. The amplification by the non-resonant instability may lead in the most extreme cases to very high amplification levels, pointing towards SNr in very early free-expansion phase as efficient CR accelerators. In that case, the magnetic density should scale as $V_{\rm sh}^3$ as pointed out by Bell (2004). This issue is of prime importance and should deserve detailed observational investigations, unfortunately difficult to perform in this SNr evolution stage. However, this early phase lasts for a very small fraction of the whole SNr lifetime except in a low density and highly magnetised medium as expected in a turbulent hot ISM phase often called as superbubbles (see for instance Parizot et al. 2004). Answering the question of the maximum CR energy expected in SNr and the origin of the CR knee at $\sim 3 \times 10^{15}$ eV requires then a time dependent CR spectrum calculation (see Ptuskin & Zirakshvili 2005) and to account for the CR diffusion regimes correctly. If the first point is beyond the scope of the present work, the second point will be discussed in Paper II.

7. Conclusion

We summarize the main results of the work as follows. Upstream of an astrophysical shock, the cosmic ray streaming triggers an instability that has two different regimes: one occurs under resonant condition and dominates the longer wavelengths of the Alfvén spectrum, the other occurs off resonance and dominates at shorter wavelengths (this is the Bell regime of the instability Bell 2004). In the purpose of investigating the turbulent transport of the highest energy cosmic rays both regimes have to be considered over the remnant evolution. The non-resonant instability saturates either by non-linear transfer effects or by a quenching effect at $k_{\rm c} r_* = 1$. The saturation level is $k_\parallel S(k_\parallel) \simeq \xi_{\rm CR}(V_{\rm sh}/c)\ \mathcal{M}_{\rm A\infty}^2/(\Phi k_\parallel r_\star)$. The main saturation mechanism for the resonant instability stems from the fact that the shock front catches up with the growing waves over a diffusion length. The saturation level is modulated by the non-resonant saturation level according to: $k_\parallel S(k_\parallel) \simeq \xi_{\rm CR}\ (\mathcal{M}_{\rm A\infty}/\Phi) \times \overline{B}_{\rm n-res}/B_\infty$. The non-resonant regime of the instability dominates the resonant contribution only for very fast shock velocity.

The streaming instability partially determines the spectrum, namely its $k_\parallel$ dependence. The spectra are close to $k_\parallel^{-1}$, which, as will be shown in the second paper, can lead to a Bohm scaling for the transport of cosmic rays. The $k_\perp$ dependence of the spectrum is remodeled by the non-linear cascade of Alfvén waves, that essentially works transversally, the transfer time being short enough as compared to the advection time. The excited Alfvén turbulence constitutes the scattering medium for the cosmic rays and it would be incomplete if only the forward Alfvén waves would be present as a result of the resonant streaming instability. A second nonlinear transfer develops which is the backscattering of primary Alfvén waves off slow magneto-sonic modes, and which re-distributes the energy from the forward Alfvén waves to the backward ones and to the magneto-sonic ones. This process turns out to be unavoidable because the Alfvén speed exceed the sound speed upstream and is sufficiently fast compared to the advection time.

Some turbulent dynamo action can be expected downstream, but the intensity of the mean field should not significantly exceed the equipartition value. The turbulence is also compressed at the shock front producing reduced residence time of the relativistic particles downstream. Apart for low shock velocities, i.e. lower than 10^{-2} c, the residence time downstream is lower than the non-linear transfer time controled by the Alfvenic cascade. The turbulence spectra downstream are likely similar to those that have been formed upstream, since they correspond to stationary solutions of the turbulence equations in a mean field, according to recent developments of the theory of Alfvénic turbulence. This implies that the Bohm regime of cosmic ray transport if true upstream would also apply downstream. Regarding the magnetic turbulence in the Galaxy where a mean field imposes its constraint, a question rises about the determination of the two indices α and β of the anisotropic spectrum. They are only linked by the relation $3\alpha + 2\beta = 7$ (Galtier et al. 2005). It is reasonable to think that β and thus α are determined by shocks and thus $\beta = 1$ and $\alpha = 5/3$ (anisotropic Kolmogorov spectrum) would be ubiquitous.

Acknowledgements. One of us, G.P., acknowledges fruitful discussions with Andrew Bell and Heinrich Völk. We are also grateful to Sébastien Galtier for exchanges about the most recent understanding of Alfvénic turbulence.

Appendix A: The nonlinear operator of backscattering

The energy spectra are normalized such that $\omega^a N^a = S^a_{3\mathrm{d}}/\rho_0 V_\mathrm{A}^2$; in other words, the N^a have the dimension of an action (namely, an occupation number times $\hbar$).

$$\dot{N}^+ = -\int \frac{\mathrm{d}^3\boldsymbol{k}^-}{(2\pi)^3}\frac{\mathrm{d}^3\boldsymbol{k}^\mathrm{s}}{(2\pi)^3} w \times (N^+N^- + N^+N^\mathrm{s} - N^-N^\mathrm{s}) \quad (A.1)$$

$$\dot{N}^- = \int \frac{\mathrm{d}^3\boldsymbol{k}^+}{(2\pi)^3}\frac{\mathrm{d}^3\boldsymbol{k}^\mathrm{s}}{(2\pi)^3} w \times (N^+N^- + N^+N^\mathrm{s} - N^-N^\mathrm{s}) \quad (A.2)$$

$$\dot{N}^\mathrm{s} = \int \frac{\mathrm{d}^3\boldsymbol{k}^+}{(2\pi)^3}\frac{\mathrm{d}^3\boldsymbol{k}^-}{(2\pi)^3} w \times (N^+N^- + N^+N^\mathrm{s} - N^-N^\mathrm{s}). \quad (A.3)$$

The transition probability has been calculated by Akhiezer & Akhiezer (1975) and reads

$$w = \frac{\pi}{8} f \frac{V_\mathrm{A}^4}{\rho_0} \frac{(k_\parallel^+)^2 (k_\parallel^-)^2 (k_\parallel^\mathrm{s})^2}{\omega_+\omega_\mathrm{f}\omega_\mathrm{s}} \times (2\pi)^3 \delta(\boldsymbol{k}^+ - \boldsymbol{k}^- - \boldsymbol{k}^\mathrm{s})\delta(\omega^+ - \omega^- - \omega^\mathrm{s}) \quad (A.4)$$

with the angular factor f depends on the unitary vectors $\boldsymbol{n} \equiv \boldsymbol{k}/k$ and defined by

$$f = f(\boldsymbol{n}_+, \boldsymbol{n}_-, \boldsymbol{n}_\mathrm{s}) \equiv \frac{((\boldsymbol{n}_+ \times \boldsymbol{e}_b)\cdot(\boldsymbol{n}_- \times \boldsymbol{e}_b))^2}{(n_+^\perp)^2 (n_-^\perp)^2} \quad (A.5)$$

where $\boldsymbol{e}_b$ is the unitary vector in the direction of the mean field $\boldsymbol{B}_o$. The transition probability w can be rewritten in the following way:

$$w = \frac{\pi}{8} f \frac{|\cos\theta_-|}{\beta_\mathrm{s}\rho_0} k_\parallel^+ |k_\parallel^-| k_\parallel^\mathrm{s} (2\pi)^2 \delta(\boldsymbol{k}_\perp^+ - \boldsymbol{k}_\perp^- - \boldsymbol{k}_\perp^\mathrm{s}) \times 2\pi\delta\left(k_\parallel^+ - k_\parallel^\mathrm{s}\frac{1+\beta_\mathrm{s}}{2}\right)\delta\left(k_\parallel^- + k_\parallel^s\frac{1-\beta_\mathrm{s}}{2}\right).$$

The last product of the two δ-functions can be written under several convenient forms for the calculation of the various integrals. The control parameter κ (Eq. (45)) rises after multiplying the nonlinear operator kernel by the advection time τ_a (Eq. (17)). Furthermore, assuming unmodified transverse spectra of the form $k_\perp^{-q}$ with $q > 2$, when we writes the system for S^+, S^- and S^s, in term of the variable y, it can be realized that it is scale invariant. Assuming power law solutions for the S's, the coefficients of the system are independent of the wave vectors after integrating over the angles. Because of the integration of the delta-functions over the k's, the system is reduced to a differential system involving three 1D-spectra depending on a single wavenumber $k_\parallel$, since $k_\parallel^- \simeq -k_\parallel^+$ and $k_\parallel^\mathrm{s} \simeq 2k_\parallel^+$. Before writing the differential system, we approximate the theory specifically for the case $y < 1$, where we have already seen that the spatial variation of the rms magnetic field is smooth compared to e^{-y} and we fix $\overline{B}$ at its value B_0 at the shock front and introduce the amplification factor $A \equiv B_0/B_\infty$. We set $N = X(y)N_*$ for the three spectra, where we introduce N_* such that $S_*(k_\parallel)2\pi(q-2)l^2(k_\perp l)^{-q} = k_\parallel V_{\mathrm{A}\infty} N_*(k_\parallel)/\rho_0 V_{\mathrm{A}\infty}^2$.

The evolution system accounts for the case of substantial pre-amplification by the non-resonant instability. The third-order evolution system reads as

$$(X^+ + X^-)\frac{\partial X^+}{\partial y} = -\mathrm{e}^{-y}X^+ + A\kappa \times [X^+X^- + (X^+ - X^-)X^\mathrm{s}] \quad (A.6)$$

$$(X^+ + X^-)\frac{\partial X^-}{\partial y} = \mathrm{e}^{-y}X^- - A\kappa \times [X^+X^- + (X^+ - X^-)X^\mathrm{s}] \quad (A.7)$$

$$(X^+ + X^-)\frac{\partial X^\mathrm{s}}{\partial y} = -\frac{A\kappa}{2} \times [X^+X^- + (X^+ - X^-)X^\mathrm{s}]. \quad (A.8)$$

For $\kappa = 0$, the ratio of the first two equations leads to $X^+X^- =$ constant $= X^+(y=1)X^-(y=1)$.

Appendix B: A more complete nonlinear theory

Because of the efficiency of the backscattering process when $\kappa \sim 1$, it is reasonable to envisage a secondary generation of backward sound waves from backward Alfvén waves, which also regenerates the forward Alfvén spectrum: $A^- \to A^+ + S^-$.

$$\dot{N}^- = -\int \frac{d^3\boldsymbol{k}^+}{(2\pi)^3} \int \frac{d^3\boldsymbol{k}^s}{(2\pi)^3} w \times (N^- N^+ + N^- N^{s-} - N^+ N^{s-}) \tag{B.1}$$

$$\dot{N}^+ = \int \frac{d^3\boldsymbol{k}^-}{(2\pi)^3} \int \frac{d^3\boldsymbol{k}^s}{(2\pi)^3} w \times (N^- N^+ + N^- N^{s-} - N^+ N^{s-}) \tag{B.2}$$

$$\dot{N}^{s-} = \int \frac{d^3\boldsymbol{k}^+}{(2\pi)^3} \int \frac{d^3\boldsymbol{k}^-}{(2\pi)^3} w (N^- N^+ + N^- N^{s-} - N^+ N^{s-}). \tag{B.3}$$

We combine the primary and the secondary process, include damping of the stable waves (actually the backward waves are damped by the cosmic ray streaming at the same rate as the forward waves are amplified). The damping rate of the sound waves is $\sqrt{\frac{\pi}{8}\frac{m_e}{m_i}} k_\parallel c_s$. We proceed as in the previous appendix to describe the nonlinear evolution of the resonant instability, and found that the spectra proportional to S_* are still recovered. We then form the four order differential system on the amplitudes of the spectra that governs the y-profiles:

$$(X^+ + X^-)\frac{\partial X^+}{\partial y} = -e^{-y} X^+ - A\kappa \times (X^- - X^+)(X_s^+ + X_s^-) \tag{B.4}$$

$$(X^+ + X^-)\frac{\partial X^-}{\partial y} = e^{-y} X^- + A\kappa \times (X^- - X^+)(X_s^+ + X_s^-) \tag{B.5}$$

$$(X^+ + X^-)\frac{\partial X_s^+}{\partial y} = g_s X_s^+ - A\frac{\kappa}{2} \times (X^- X^+ + X^+ X_s^+ - X^- X_s^+) \tag{B.6}$$

$$(X^+ + X^-)\frac{\partial X_s^-}{\partial y} = g_s X_s^- - A\frac{\kappa}{2} \times (X^- X^+ + X^- X_s^- - X^+ X_s^-). \tag{B.7}$$

In the case $\varepsilon = 0$, g_s is a pure number: $g_s = A\frac{2}{3}\sqrt{\frac{\pi}{8}\frac{m_e}{m_i}}\frac{cc_s}{V_{sh}^2}$ which has to be compared with κ; typically $g_s \sim (10^{-3}$–$10^{-2})\kappa$. It turns out that a relaxation of the sound waves is possible only for $g_s^2 > \kappa^2(X^+ - X^-)^2$, which implies $X^+ \simeq X^-$.

References

Akhiezer, A., Akhiezer, I. A., Polovin, R. V., Sitenko, A. G., & Stepanov, K. N. 1975, Plasma Electrodynamics, Nonlinear Theory and Fluctuations (Oxford: Pergamon Press), Vol. 2

Bell, A. R. 2004, MNRAS, 353, 550

Bell, A. R., & Lucek, S. G. 2001, MNRAS, 321, 433

Berezhko, E. G., & Ellison, D. C. 1999, ApJ, 526, 385

Berezhko, E. G., & Völk, H. J. 2004, A&A, 419, L27

Berezhko, E. G., Elshin, V. K., & Ksenofontov, L. C. 1996, JETP, 82, 1

Bhattacharjee, A., & Ng, C. S. 2001, ApJ, 548, 318

Casse, F., Lemoine, M., & Pelletier, G. 2002, Phys. Rev. D, 65, 023002

Drury, L. O'C., Ellison, D. E., Aharonian, F. A., et al. 2001, SSR, 99, 329

Cho, J., & Vishniac, E. T. 2000, ApJ, 539, 273

Galtier, S., Nazarenko, S. V., Newell, A. C., & Pouquet, A. 2000, J. Plasma Phys., 63, 447

Galtier, S., Pouquet, A., & Mangeney, A. 2005, Physics of Plasma, 12, 092310

Goldreich, P., & Shridar, S. 1995, ApJ, 438, 763

Goldreich, P., & Shridar, S. 1997, ApJ, 485, 680

Iroshnikov, P. S. 1964, Soviet Astronomy, 7, 566

Kraichnan, R. H. 1965, Phys. Fluids, 8, 1385

Lerche, I. 1967, ApJ, 147, 689

McKenzie, J. F., & Völk, H. J. 1982, A&A, 116, 191

Marcowith, A., Lemoine, M., & Pelletier, G. 2006, A&A, 453, 193 (Paper II)

Maron, J., & Goldreich, P. 2001, ApJ, 554, 1175

Melrose, D. B. 1986, Instabilities in space and laboratory plasmas (Cambridge University Press)

Moffatt, H. K. 1978, Magnetic filed generation in electrically conducting fluids (Cambridge University Press)

Parizot, E., Marcowith, A., van der Swaluw, E., Bykov, A. M., & Tatischeff, V. 2004, A&A, 424, 747

Parizot, E., Marcowith, A., Ballet, J., & Gallant, Y. A. 2006, A&A, [arXiv:astro-ph/0603723]

Pelletier, G., & Kersalé, E. 2000, A&A, 361, 788

Pohl, M., Yan, H., & Lazarian, A. 2005, ApJ, 626, L101

Ptuskin, V. S., & Zirakashvili, V. N. 2003, A&A, 410, 189

Ptuskin, V. S., & Zirakashvili, V. N. 2005, A&A, 429, 755

Schlickheiser, R., & Vainio, R. 1998, A&A, 331, 793

Skilling, J. 1975, MNRAS, 172, 557; 173, 245

Vink, J. 2004, Adv. Space Sci., 33, 356

Völk, H. J., Berezhko, E. G., & Ksenofontov, L. T. 2005, A&A, 433, 229

Wentzel, D. G. 1969, ApJ, 156, 303